Available online at www.sciencedirect.com
ScienceDirect
Journal of Molecular Catalysis A: Chemical 264 (2007) 33–39
JOURNAL OF MOLECULAR CATALYSIS A: CHEMICAL
www.elsevier.com/locate/molcata

Interaction of mordenite with an aromatic hydrocarbon: An embedded ONIOM study

Bavornpon Jansang [a,b], Tanin Nanok [a,b], Jumras Limtrakul [a,b,*]

[a] *Laboratory for Computational and Applied Chemistry, Department of Chemistry, Faculty of Science, Kasetsart University, Bangkok 10900, Thailand*
[b] *Center of Nanotechnology, Kasetsart University Research and Development Institute, Kasetsart University, Bangkok 10900, Thailand*

Received 7 May 2006; received in revised form 26 June 2006; accepted 26 June 2006
Available online 9 October 2006

Abstract

The structure of mordenite (MOR) and its interaction with benzene has been investigated within the framework of our-own-N-layered integrated molecular orbital + molecular mechanics (ONIOM) approach utilizing the two-layer ONIOM scheme (B3LYP/6-31G(d,p):UFF). The effect of the long range interactions is also included via optimized point charges added to the ONIOM2(B3LYP/6-31G(d,p):UFF), embedded ONIOM. Inclusion of the extended zeolitic framework covering the nanocavity has an effect on the adsorption properties. The adsorption energies estimated from 3T and 12T quantum clusters of −6.0 and −6.9 kcal/mol, respectively, are significantly lower than that obtained from the 120T ONIOM2 scheme of −16.6 kcal/mol. The completed adsorption model obtained at the embedded ONIOM2(MP2/6-31G(d,p):UFF) method predicts the adsorption energy of −23.4 kcal/mol, which is comparable to the van der Waals-corrected periodic calculation adsorption energy of −21.5 kcal/mol.

Keywords: Mordenite; Benzene adsorption; ONIOM; Embedded ONIOM

1. Introduction

Zeolites are solid catalysts which are environmentally friendly and widely used in petrochemical processes [1,2] due to their high activity and selectivity. Among many types of zeolites of commercial interest, mordenite (MOR) is one of the most important ones. In particular, its protonic form, which can be equivalent to a proton donor, has received attention to serve as the catalyst in many reaction processes, including the catalytic dewaxing, *n*-paraffin cracking, and isomerization of hydrocarbons [3–5].

Because of its importance in catalysis and separation processes, the acidity of H-MOR zeolite has been extensively studied by various techniques such as XPS, NMR, TPD, IR and thermobalance [6–8]. However, the acidity of the hydroxyl groups located in different structural environments cannot easily be determined by experiment. Furthermore, the problems of the homogeneity or heterogeneity of the Si–OH–Al groups and of their location in the structure of H-MOR have been discussed by many authors [6–8], but a satisfactory solution has yet to be found. Alberti [9] has located Brønsted acid sites in the crystal structure of H-MOR using crystallochemical and IR spectroscopic data and reported that about 2/3 of the acid sites are in the larger channels and 1/3 in the smaller channels, which agrees with the relative intensities of the high frequency (HF) and low frequency (LF) OH-bands.

Although, there are many theoretical calculations [10–14] on Brønsted acid sites in MOR, the results obtained so far have not yet led to a conclusive description. Moreover, the acidity itself cannot be determined by characterizations of the solid acid alone, but must be investigated by the interaction of the probe molecule with the acid site. The characterization of the acid-base properties of protonic and cationic zeolite using benzene as a probe molecule has been reported in a series of papers [15,16]. Recently, different adsorption geometries of benzene in H-MOR have been investigated for several acid sites using the periodic density functional theory (DFT) calculation and these have shown that the adsorption strength is correlated to the deformation of the local acidic adsorption site [12]. The calculated adsorption energies were, however, significantly underestimated in comparison to the experimental values. This is due to the fact that the density functional theory

* Corresponding author. Tel.: +662 9428900x323; fax: +662 9428900x324.
E-mail address: fscijrl@ku.ac.th (J. Limtrakul).

1381-1169/$ – see front matter © 2006 Elsevier B.V. All rights reserved.
doi:10.1016/j.molcata.2006.06.054

does not sufficiently describe the short-range van der Waals interactions, which mainly contribute to the adsorption process of non-polar hydrocarbons. In order to include the dispersive contribution, one can use the more general our-own-N-layered integrated molecular orbital + molecular mechanics (ONIOM) method by taking advantage of its combination of different levels of calculation. In previous work [17], we studied the confinement effects on the adsorption of aromatic hydrocarbons on industrially important zeolitic nanocatalysts. It was found that the combination of the B3LYP density functional theory, as an accurate treatment of the interactions of adsorbed molecules with the acid site of zeolite, and the universal force fields (UFF) for inclusion of the van der Waals (vdW) interactions, provided quite satisfactory results for the adsorption energies as compared to the experimental data. In addition, this scheme has also been demonstrated to yield adsorption energies close to the experimental estimates for other systems [18–21]. We thus expect that, in the case of the interaction of H-MOR with benzene, this ONIOM scheme should also be successful.

In this study, the locations of the Brønsted acid site as well as the adsorption of benzene in H-MOR are studied. In addition to the ONIOM method, for more accurate calculations, the layer of point charges representing an electrostatic long-range interaction Madelung potential of the entire zeolite lattice is added, and is called embedded ONIOM.

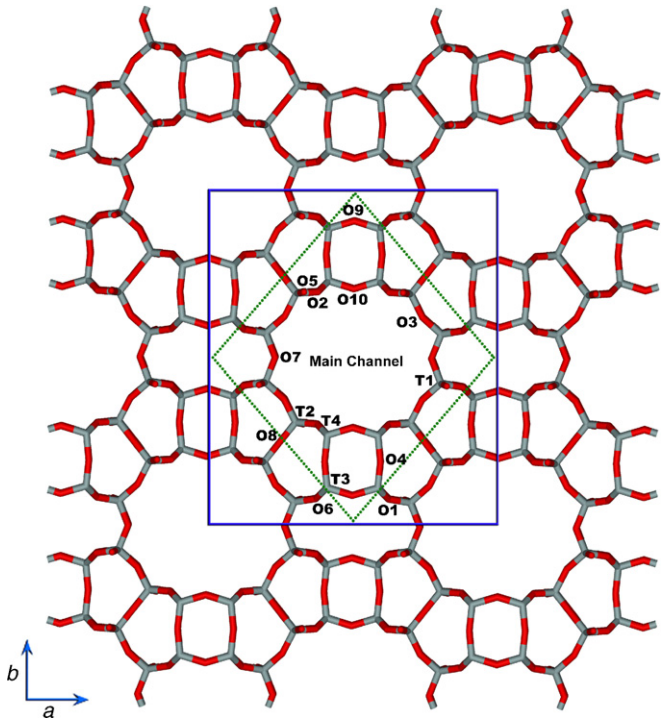

Fig. 1. Projection of mordenite framework along the main 12-membered ring channel, *c*-direction. The solid frame shows the conventional centrosymmetric orthorhombic unit cell, the dashed frame the primitive unit cell.

2. Methodology

The crystal lattice structure of MOR was generated by using the Cerius[2] program in [0 0 1] direction. The topology is an orthorhombic space group *Cmcm* with unit cell parameters $a = 18.09$ Å, $b = 20.52$ Å and $c = 7.52$ Å [22]. The framework system consists of two types of one-dimensional channel: the 12- and 8-membered ring (MR) channels, running parallel to the *c*-axis (see Fig. 1). The main 12 MR channels with an elliptical section of 6.5×7.0 Å are perpendicularly interconnected by the eight-ring side pockets of 2.6 Å $\times$ 5.7 Å in diameter, running along the *b*-axis. In the framework system of MOR, there are four inequivalent tetrahedral sites (T1, . . ., T4) and 10 oxygen sites (O1, . . ., O10).

In order to study the structural stability of Brønsted acid sites of H-MOR, in the present study, we have followed the work of Alberti [9] and focused only on the T-sites in the main 12 MR channel (T1, T2, and T4). This is reasonable since many chemical reactions occur only in the main 12MR channels, due, e.g., here to the relative sizes of the benzene molecule and the channel system. Therefore, only six Brønsted acid sites (Al(T1)O3H, Al(T1)O7H, Al(T2)O2H, Al(T2)O3H, Al(T4)O2H, and Al(T4)O10H) in the main 12 MR channel are considered as the accessible sites for the benzene molecule.

The two-layer ONIOM scheme is employed to examine the energetically most favorable location of the Brønsted acid sites of H-MOR. For computational efficiency, only the small active region is treated accurately with the density functional theory method, while the contribution of interactions from the rest of the model is approximated by a less expensive method. The B3LYP/6-31G(d,p) level of theory is applied for the 12T tetrahedral quantum cluster, which is considered to represent the active site of H-MOR. The remainder of the 108T extended framework connecting the 12T active site is treated with the universal force field (UFF) [23] to reduce the computational time and to practically represent the confinement effect of the zeolite pore structure. This force field has been found to provide a good description of the short-range van der Waals intereactions between the sorbate molecules and zeolitic wall [18–21]. During the geometry optimization, only the active site region of the 3T tetrahedral cluster, [≡SiO(H)AlOSi≡], is allowed to relax while the remainder is fixed at the crystallographic coordinates. The results show that the introduction of a proton to the bridging O2 connected to the T2 site provides the energetically most stable Brønsted acid site, Al(T2)O2H, which is in good agreement with the experimental observation reported by Alberti [9]. The energy difference between the most stable and the least stable sites is 26.5 kcal/mol. The large difference in the relative energy may be due to the use of the small active site, [≡SiO(H)AlOSi≡], which is allowed to relax during the optimization. The stability increases in order Al(T1)O7H < Al(T1)O3H < Al(T4)O10H.) < Al(T4)O2H < Al(T2)O3H < Al(T2)O2H. These results are, however, slightly different from the periodic density functional theory calculations of Bucko et al. [10] and Demuth et al. [11].

The most stable model of the Brønsted acid sites obtained from the geometry optimization, Al(T2)O2H, is then used for studying the interaction energy of benzene on H-MOR. The benzene molecule is treated with the same level of theory used for the 12T active site (B3LYP/6-31G(d,p)) and freely relaxed during the optimization.

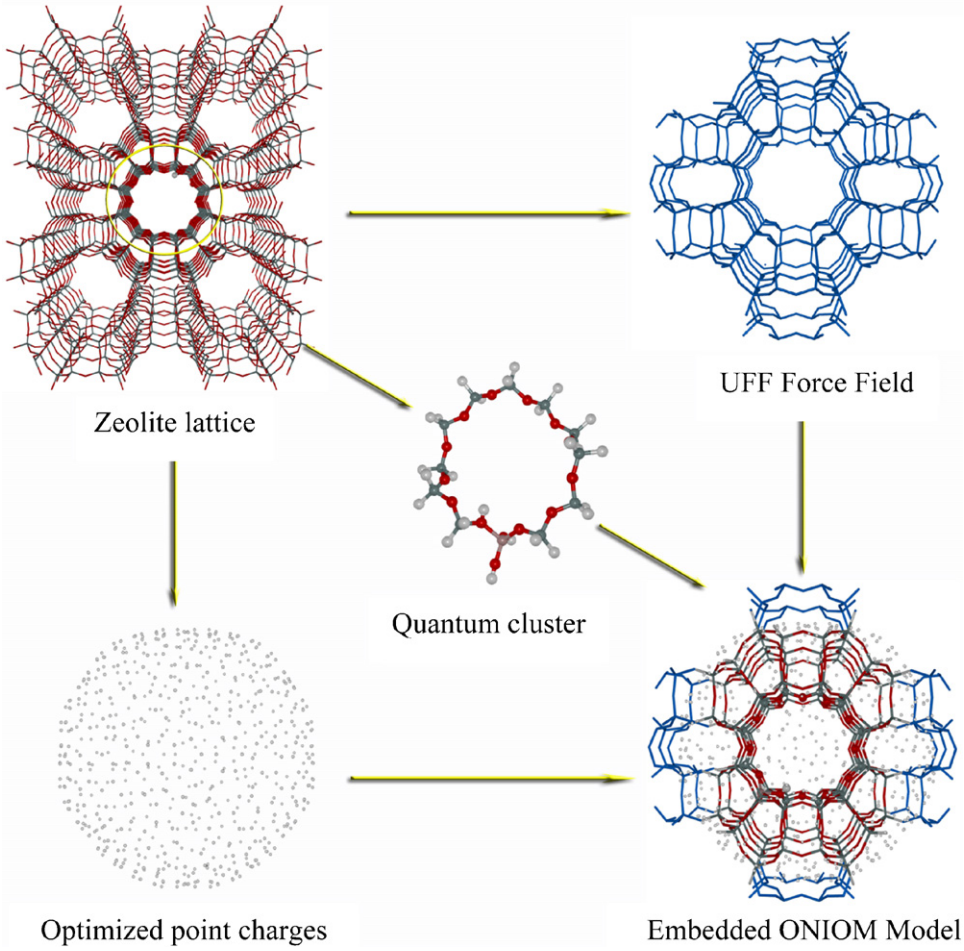

Fig. 2. Schematic diagram of the embedded ONIOM method.

In order to achieve the full description of the adsorption properties of probe molecules in zeolitic pores, it is necessary to take into account the long-range interactions of the extended framework, which is important for adsorption–desorption in zeolites. The Madelung potential from the zeolite lattice beyond the 12T cluster was introduced by using the newly developed approach called "embedded ONIOM2" [24,25]. This model is subdivided into three parts. The inner part (catalytic center) is a 12-tetrahedral (12T) quantum cluster representing for the active site. The second part is the universal force field accounting the confinement effect of the zeolitic pore. The outermost part of the model is a set of optimized point charges representing the remaining Madelung potential generated from the infinite zeolite lattice. The schematic diagram of our embedded ONIOM model for MOR is graphically illustrated in Fig. 2. In order to obtain more reliable interaction energies, the single point energy calculation at MP2/6-31G(d,p):UFF//B3LYP/6-31G(d,p):UFF corrected for the basis set superposition errors (BSSE) is carried out. All calculations have been performed on the modern linux workstation using the Gaussian98 code [26].

3. Results and discussion

It is not surprising that the use of small cluster models representing the active site of zeolites can provide an appreciable description of the interaction between small adsorbing molecules and zeolites [27–29]. This is, however, not the case for studying the adsorption of bulky aromatic hydrocarbons, like benzene, in the zeolite pores because the interaction energy is not only described by the interaction between the adsorbing molecule and the local acid site, but also the interaction between the adsorbing molecule and the zeolitic wall. Therefore, the environment surrounding the local active site will affect the adsorption process of benzene on H-MOR zeolite. In this study, four models of the active site of the Al(T2)O2H site, 3T quantum cluster, 12T quantum cluster, 120T ONIOM2, and the embedded 120T ONIOM2 model (see Fig. 3), are demonstrated. As mentioned in the methodology section, only atoms in the quantum cluster part representing the Brønsted acid site, [≡SiO(H)AlOSi≡], are allowed to relax, while the rest are fixed at the crystallographic coordinates during the geometry optimization.

3.1. Comparisons of geometrical structures for different bare zeolite models

The selected geometrical structures for all cluster models are documented in Table 1. The extension of the local active site up to the 12T quantum cluster gives rise to the lengthening of

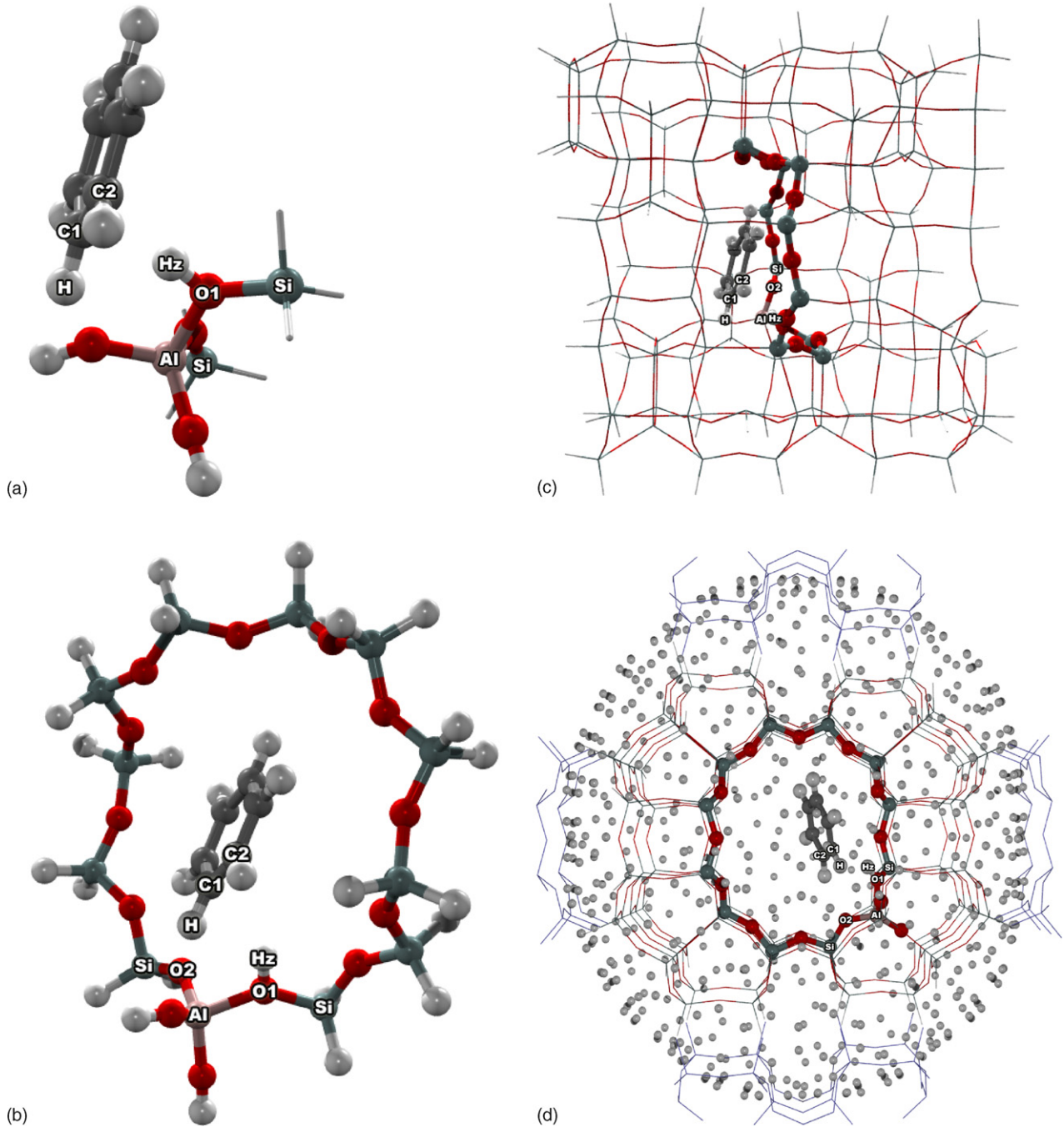

Fig. 3. Optimized geometries of the [C_6H_6/H-MOR] adsorption complex using (a) 3T, (b) 12T, (c) 120T and (d) embedded 120T cluster models, respectively.

the O–Hz bond distance by 0.4 pm (96.7 and 97.1 pm for the 3T and 12T cluster, respectively). The increment of the O–Hz bond distance suggests that the 12T quantum cluster is more acidic than the 3T quantum cluster and, thus, might lead to the expected higher adsorption energy of benzene. All other selected parameters are slightly decreased, by 1.1–2.4 pm and 0.2 ° for the bond distances and the bond angle, respectively. The short-range van der Waals interactions from the extended framework included in the ONIOM2(B3LYP/6-31G(d,p):UFF) model was found to have only a small effect on the local geometry of the acid site. The protonation at the O1 site results in the contraction of the Si–O1 and Al–O1 bonds and the elongation of the Al–O2 bond compared with the 12T quantum cluster (see Table 1). The Si–O1–Al bond angle increases by 1.2 ° from the 12T cluster model (132.9 ° versus 134.1 °). With the inclusion of long-range electrostatic interactions from the zeolitic lattice in the "embedded ONIOM2" model, significant changes of the structural active site can be observed, i.e., the Al–O1 and Al–O2 bond distances increase by 6.6 and 1.2 pm, the Si–O1 bond distance decreases by 2.9 pm, and the Si–O1–Al bond angle increases by 2.0 ° in comparison to the "native ONIOM" model. The most realistic model, the embedded OINIOM2 model, elongates the O1–Hz bond distance (Brønsted acid site) by 0.2 pm (97.2 versus 97.0 pm). Further support for the reliability of our active

Table 1
Optimized structural parameters (distances in pm and bond angles in degrees) for H-MOR zeolite, C_6H_6 and the [C_6H_6/H-MOR] adsorption complex using the 3T, 12T, 120T and embedded 120T models

Parameters	Models							
	3T[a]		12T[a]		120T[b]		Embedded 120T[b]	
	Bare cluster	Complex	Bare cluster	Complex	Bare cluster	Complex	Bare cluster	Complex
Distances								
O1–Hz	96.7	98.0	97.1	97.8	97.0	97.6	97.2	98.3
Si–O1	169.5	169.4	168.4	168.2	165.7	165.9	162.8	162.8
Al–O1	188.9	187.3	186.5	185.4	188.6	187.2	195.2	192.6
Al–O2	167.6	167.2	166.3	167.0	163.8	164.0	165.0	165.1
Al···Hz	238.9	236.7	235.1	240.5	238.2	238.7	237.2	238.6
C1···Hz	–	223.4	–	248.0	–	258.8	–	244.1
C2···Hz	–	235.2	–	283.1	–	323.0	–	286.9
C1–C2	139.6	140.1	139.6	140.1	139.6	139.9	139.6	140.1
C1–H	108.6	108.6	108.6	108.9	108.6	108.6	108.6	108.7
Angles								
∠Si–O1–Al	133.1	132.3	132.9	132.0	134.1	132.8	136.1	134.7

[a] Optimized at the B3LYP/6-31G(d,p) level of theory.
[b] Optimized at the ONIOM2(B3LYP/6-31G(d,p):UFF) level of theory.

site subunit, ≡Si–OH–Al≡, is given by NMR studies. Klinowski et al. have estimated the internuclear distance between the aluminum and proton nuclei in the Brønsted acid site, Al···Hz, of different zeolites [30,31] to be in the range of 234–252 pm, and our computed Al···Hz distances of the realistic model of 120T-H-MOR zeolite is 237.2 pm.

Despite the small magnitude of the changes in the distances and angles at the active region with the ONIOM model, we expect to be able to detect how the adsorption properties of the probe molecule on the zeolite will be affected by the presence of the confinement effect and the long-range interactions from the zeolite framework. This will be discussed in the following section.

3.2. Interaction of benzene with acidic mordenite zeolite

The B3LYP/6-31G(d,p) level of theory predicts the C–C and C–H bond lengths of isolated benzene of 139.6 and 108.6 pm, respectively, which are in excellent agreement with the experimental observation of 139.7 and 108.4 pm for C–C and C–H bond lengths, respectively. The changes of geometrical parameters upon the adsorption of benzene are in accordance with Gutmann's rule [32,33], i.e., a lengthening of the O1–Hz bond along with a corresponding slight decrease in the Al–O1 bond and lengthening of the Al–O2 bond. The O–Hz bond length of the active region increases by about 1.3, 0.7, and 0.7 pm for the 3T, 12T, and 120T cluster models, respectively, from the isolated zeolite. The adsorption complexes show a slight elongation of the C–C bond length as compared to the isolated molecule, however, no significant change is observed in the length of the C–H bonds (see Table 1). The distances between the benzene molecule and the Brønsted proton increase as the cluster size is increased. This reflects the accessibility of the local active site to the adsorbing molecules. Since the benzene molecule is comparatively large as compared to the pore size of mordenite zeolite, it is not possible for the 12T and 120T complexes to come as close to the Brønsted acid site as the 3T cluster model. This is due to the steric hindrance of the benzene molecule and the environment surrounding the local acid site. Furthermore, the zeolitic wall included in the 120T cluster model was found to have an effect on elongating the separation of the benzene molecule and the acid site. The shortest distances between the carbon atom of benzene and the Brønsted proton of zeolite (C···Hz) are calculated to be 223.7, 248.0, and 258.8 pm for the 3T, 12T, and 120T cluster models, respectively.

The electrostatic interactions from the zeolitic framework included in the embedded ONIOM2 model have significant effects on enhancing the interaction of benzene and the active site. The benzene molecule comes closer to the acid site and thus resulting in the longer O–Hz bond distance as compared to the 12T and 120T cluster models. The shortest C···Hz distance and the O-Hz bond distance are calculated to be 244.1 and 98.3 pm, respectively. All selected parameters of the benzene/H-MOR adsorption complexes are documented in Table 1.

Table 2
Interaction energies (ΔE_{ads}) of the [C_6H_6/H-MOR] complex obtained from various models and methods

Models	Methods	ΔE_{Ads} (kcal/mol)
3T	B3LYP/6-31G(d,p)	−6.0
12T	B3LYP/6-31G(d,p)	−6.9
120T	ONIOM2(B3LYP/6-31G(d,p):UFF)	−16.6
Embedded 120T	Embedded ONIOM2(B3LYP/6-31G(d,p):UFF)	−22.2 (−23.4)[a]

[a] Single point energy calculation at ONIOM2(MP2/6-31G(d,p):UFF) with the BSSE correction.

The calculated adsorption energies of benzene in different H-MOR models are documented in Table 2. The adsorption energy increases with the increase of the cluster size. For the 3T and 12T cluster models, the adsorption energies are estimated to be −6.0 and −6.9 kcal/mol, respectively, at B3LYP/6-31G(d,p) level of theory, which are significantly lower than that obtained from the ONIOM2(B3LYP/6-31G(d,p):UFF) model of −16.6 kcal/mol. The large deviation of adsorption energies observed in the 3T and 12T models is due to the use of small cluster models which neglect the environmental short-range interactions, which are responsible for the confinement effect of the zeolitic pores.

The energy calculation optimized at the embedded ONIOM2(B3LYP/6-31G(d,p):UFF) predicts the adsorption energy of benzene on H-MOR to be −22.2 kcal/mol. Obviously, the DFT method does not describe the dispersive contribution properly, therefore, to obtain a more reliable adsorption energy of the embedded ONIOM2 model, the single point energy calculation at MP2/6-31G(d,p):UFF//B3LYP/6-31G(d,p):UFF corrected for the BSSE was carried out. This correction procedure yields the adsorption energy of −23.4 kcal/mol, which is comparable with the estimate value rescaled to the framework density of mordenite zeolite of nearly −21.5 kcal/mol [12]. These results indicate that our newly developed embedded ONIOM2 scheme is one of the best and a sufficient approach for studying the adsorption properties of aromatic hydrocarbons in the large extended framework zeolites.

4. Conclusions

The interaction energies of an aromatic hydrocarbon on H-MOR zeolite have been investigated with various cluster sizes and methods. We have shown that the adsorption process of aromatic hydrocarbons in zeolites cannot be described by only using the small cluster models but must also take into account the environment surrounding the local active site. The bare 3T and 12T B3LYP/6-31G(d,p) quantum clusters predict the binding energies of the [C_6H_6/H-MOR] complex of −6.0 and −6.9 kcal/mol, respectively. The effects of the zeolite framework were investigated using the ONIOM2 scheme. We found that the zeolite environment significantly enhances the adsorption energies of benzene to the zeolite. The ONIOM approach, 120T ONIOM2(B3LYP/6-31G(d,p):UFF) predicts the adsorption energy of −16.6 kcal/mol. The full description of the adsorption of adsorbing molecules in the zeolite pores was established. The lack of the van der Waals (vdW) forces in the DFT method was overcome by using the more accurate method of the MP2 level of theory, and the electrostatic Madelung potential from the extended framework was included by using the newly developed embedded ONIOM2 scheme. The predicted adsorption energy derived by this procedure corrected for the BSSE of −23.4 kcal/mol is reasonably close to the estimated value of −21.5 kcal/mol. Therefore, the results obtained in the present study suggest that the embedded ONIOM method provides a more accurate approach for studying the adsorption of aromatic hydrocarbons on this zeolite.

Acknowledgements

This work was supported in part by grants from the Thailand Research Fund (TRF Senior Research Scholar to JL) and the Kasetsart University Research and Development Institute (KURDI), as well as the Ministry of University Affairs under the Science and Technology Higher Education Development Project (MUA-ADB funds). The support from the National Nanotechnology Center (NANOTEC, Thailand) is also acknowledged.

References

[1] C.R.A. Catlow, Modeling of Structure and Reactivity in Zeolites, Academic Press, San Diego, 1992.
[2] R.A. van Santen, G.J. Kramer, Chem. Rev. 95 (1995) 637.
[3] Mobil Oil Corporation, US Patent 4,419,220, 1983.
[4] A. Dyer, A.P. Singh, Zeolite 8 (1988) 242.
[5] S. van Donk, A. Broersma, O.L.J. Gijzeman, J.A. van Bokhoven, J.H. Bitter, K.P. de Jong, J. Catal. 204 (2001) 272.
[6] H. Stach, J. Jänchen, H.G. Jerschkewitz, U. Lohse, P. Parlitz, B. Zibrowius, M. Hunger, J. Phys. Chem. 96 (1992) 8473.
[7] H. Stach, J. Jänchen, H.G. Jerschkewitz, U. Lohse, P. Parlitz, B. Zibrowius, M. Hunger, J. Phys. Chem. 96 (1992) 8480.
[8] M.J. van Niekerk, J.C.Q. Fletcher, C.T. O'Connor, J. Catal. 138 (1992) 150.
[9] A. Alberti, Zeolite 19 (1997) 411–415.
[10] T. Bucko, L. Benco, T. Demuth, J. Hafner, J. Chem. Phys. 17 (2002) 7295.
[11] T. Demuth, J. Hafner, L. Benco, H. Toulhoat, J. Phys. Chem. B 104 (2000) 4593.
[12] T. Demuth, L. Benco, J. Hafner, H. Toulhoat, F. Hutschka, J. Chem. Phys. 114 (2001) 3703.
[13] N. Jiang, S. Yuan, J. Wang, H. Jiao, Z. Qin, Y.W. Li, J. Mol. Catal. A 220 (2004) 221.
[14] S. Yuan, J. Wang, Y. Li, S. Peng, J. Mol. Catal. A 175 (2001) 131.
[15] B.L. Su, J. Chem. Soc. Faraday Trans. 93 (1997) 1449.
[16] B.L. Su, V. Norberg, Langmuir 16 (2000) 6202.
[17] R. Rungsirisakun, B. Jansang, P. Pantu, J. Limtrakul, J. Mol. Struct. 733 (2005) 239.
[18] S. Kasuriya, S. Namuangruk, P. Treesukol, M. Tirtowidjojo, J. Limtrakul, J. Catal. 219 (2003) 19357.
[19] S. Namuangruk, P. Pantu, J. Limtrakul, J. Catal. 225 (2004) 523.
[20] W. Panjan, J. Limtrakul, J. Mol. Struct. 654 (2003) 35.
[21] K. Bobuatong, J. Limtrakul, Appl. Catal. A: Gen. 253 (2003) 49.
[22] A. Alberti, P. Davoli, G.Z. Vezzalini, Kristallography 175 (1986) 249.
[23] A.K. Rappe, C.J. Casewit, K.S. Colwell, W.A. Goddard, W.M. Skiff, J. Am. Chem. Soc. 114 (1992) 10024.
[24] V. Dungsrikaew, J. Limtrakul, K. Hermansson, M. Probst, Int. J. Quan. Chem. 96 (2004) 17.
[25] B. Boekfa, J. Sirijareansre, P. Pantu, J. Limtrakul, Stud. Surf. Sci. 154 (2004) 1582.
[26] M.J. Frisch, G.W. Trucks, H.B. Schlegel, G.E. Scuseria, M.A. Robb, J.R. Cheeseman, V.G. Zakrzewski, J.A. Montgomery, R.E.Jr. Stratmann, J.C. Burant, S. Dapprich, J.M. Millam, A.D. Daniels, K.N. Kudin, M.C. Strain, O. Farkas, J. Tomasi, V. Barone, M. Cossi, R. Cammi, B. Mennucci, C. Pomelli, C. Adamo, S. Clifford, J. Ochterski, G.A. Petersson, P.Y. Ayala, Q. Cui, K. Morokuma, P. Salvador, J.J. Dannenberg, D.K. Malick, A.D. Rabuck, K. Raghavachari, J.B. Foresman, J. Cioslowski, J.V. Ortiz, A.G. Baboul, B.B. Stefanov, G. Liu, A. Liashenko, P. Piskorz, I. Komaromi, R. Gomperts, R.L. Martin, D.J. Fox, T. Keith, M.A. Al-Laham, C.Y. Peng, A. Nanayakkara, M. Challacombe, P.M.W. Gill, B. Johnson, W. Chen, M.W. Wong, J.L. Andres, C. Gonzalez, M. Head-Gordon, E.S. Replogle, J.A. Pople, Gaussian, Inc., Pittsburgh PA, 2001.
[27] S. Ketrat, J. Limtrakul, Int. J. Quant. Chem. 94 (2003) 333.
[28] J. Limtrakul, S. Jungsuttuwong, P. Khongpracha, J. Mol. Struct. 525 (2000) 153.

[29] J. Limtrakul, T. Nanok, P. Khongpracha, S. Jungsuttiwong, T.N. Truong, Chem. Phys. Lett. 349 (2001) 161.
[30] D. Frende, J. Klinoski, H. Hamden, Chem. Phys. Lett. 149 (1988) 355.
[31] J. Klinowski, Chem. Rev. 91 (1991) 1459.
[32] V. Gutmann, The Donor–Acceptor Approach to Molecular Interaction, Plenum Press, New York, 1978.
[33] V. Gutmann, G. Resch, W. Linert, Coord. Chem. Rev. 43 (1982) 133.